

Electronic Supplementary Information (ESI) for Journal of Materials Chemistry
This journal is © The Royal Society of Chemistry 2012

J. Mater. Chem.

Supporting Information

Fluoride-assisted galvanic replacement synthesis of Ag and Au dendrites on Aluminum foil with enhanced SERS and catalytic activities

Weichun Ye *^a, Yang Chen^a, Feng Zhou^b, Chunming Wang^a, Yumin Li *^c

^a Department of Chemistry and State Key Laboratory of Applied Organic Chemistry, Lanzhou University, Lanzhou 73000, China

^b State Key Laboratory of Solid Lubrication, Lanzhou Institute of Chemical Physics, Chinese Academy of Sciences, Lanzhou 730000, China

^c Key Laboratory of Digestive System Tumors, Gansu Province, 73030, China

* E-mail: yewch@lzu.edu.cn; liym@lzu.edu.cn

Electronic Supplementary Information (ESI) for Journal of Materials Chemistry
This journal is © The Royal Society of Chemistry 2012

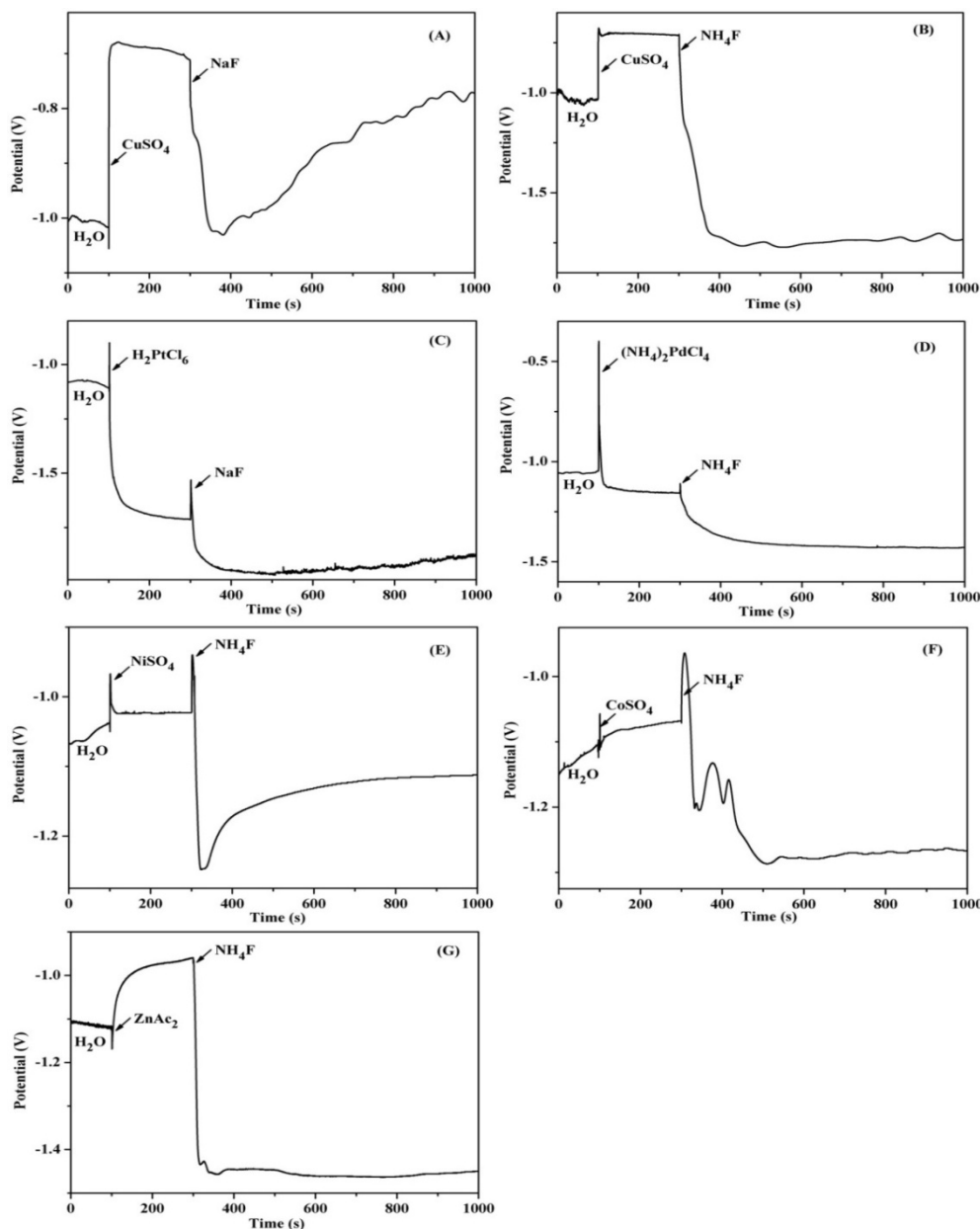


Fig. S1 OCP-t curves. The solution was only 2 ml deionized water at the beginning; 100 s later 4 ml 0.02 M metal salt solution was added fast, and then after 300 s scanning 4 ml 0.2 M NaF or NH₄F solution was added quickly. For the OCP-t curve of Zn deposition (G), the concentrations of ZnAc₂ and NH₄F were 0.1 M and 0.6 M, respectively.

Electronic Supplementary Information (ESI) for Journal of Materials Chemistry
This journal is © The Royal Society of Chemistry 2012

1. Fabrication and characterization of the thin films of Ag and Au nanoparticles

The 50 nm thickness films coated with Ag nanoparticles on blank glass sheet and Au nanoparticles on 5-7 nm thick Cr on Si(100) wafer (respectively) were obtained by electron beam evaporation. Atomic force microscopy (AFM) was used to characterize their morphologies, as shown in Fig. S-2. The AFM measurements were performed on an Agilent Technologies 5500AFM in tapping mode using a pyramidal Si tip (Veeco, RTESP). Imaging was performed under ambient condition.

The Raman spectra for the films coated with Ag and Au nanoparticles were measured under the same conditions with the as-produced Ag and Au dendrites and shown in Fig. S-3.

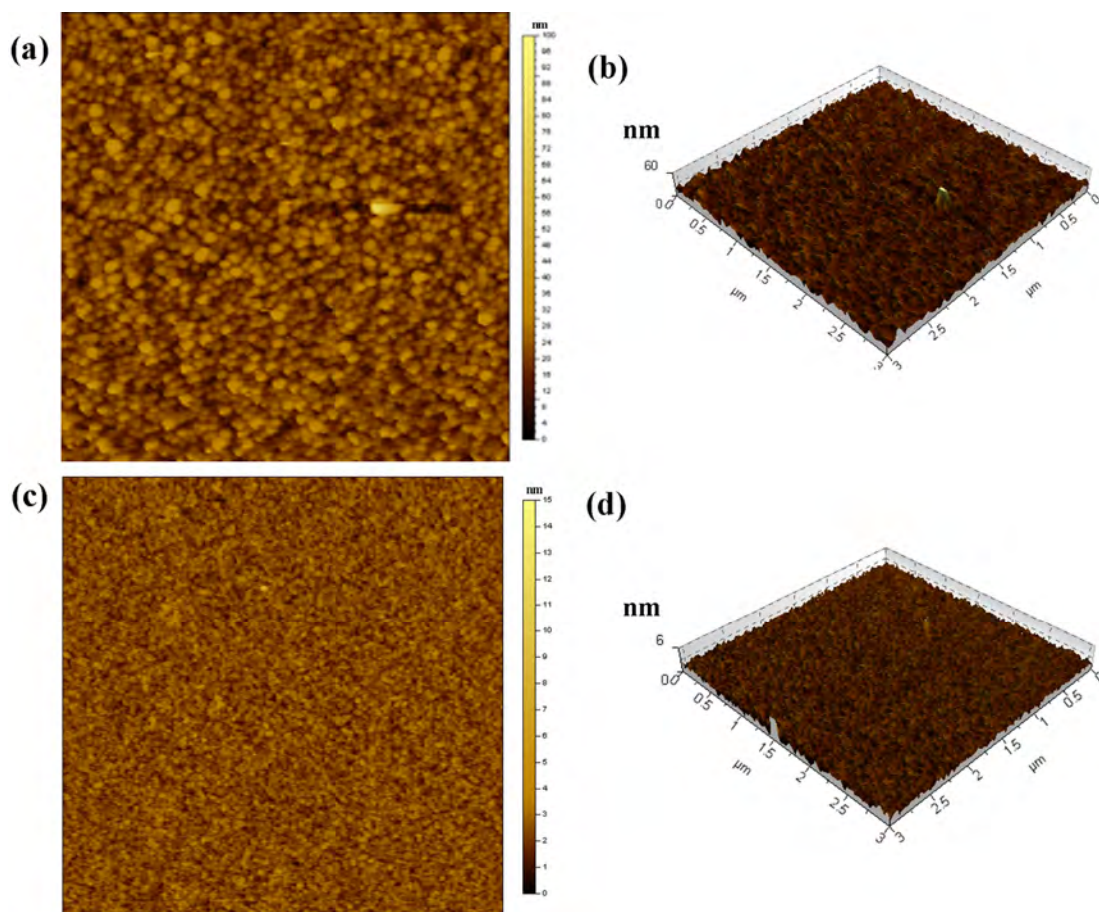


Fig. S2 The AFM images of Ag film (a and b) and Au film (c and d) obtained from electron beam evaporation.

Electronic Supplementary Information (ESI) for Journal of Materials Chemistry
This journal is © The Royal Society of Chemistry 2012

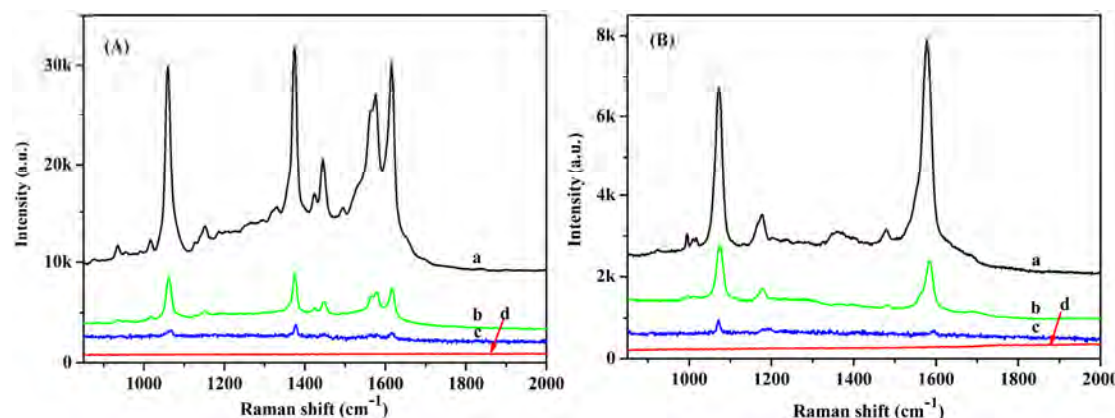


Fig. S3 The Raman spectra of 2-NAT (A) and 4-MBA (B). The ethanolic solution with 1 mM analyte was adsorbed on silver dendrites in the present study (curve a), the silver film (curve b) and gold film (curve c) obtained by electron beam evaporation, and pure Al foil (curve d).

2. EF calculation

Raman and SERS vibrational spectra preserved a close agreement; there are, however, specific changes in the relative intensity between them. Changes in relative intensity may be used to extract information about the orientation of the chemisorbed molecule at the metal surface¹. According to the method developed by Tian group², SERS enhancement factor can be calculated by the following equation:

$$EF = \left(\frac{I_{SERS}}{I_{norm}} \right) \left(\frac{N_{bulk}}{N_{surf}} \right)$$

where I_{SERS} , I_{norm} , N_{bulk} , and N_{surf} are the measured SERS intensity for a monolayer of scatterers, the measured intensity of nonenhanced or normal Raman scattering from a bulk sample, the number of molecules under laser illumination for the bulk sample, and the number of molecules in the SAM, respectively.

The N_{bulk} and N_{surf} values are calculated on the basis of the estimate of the concentration of surface species or bulk sample and the corresponding sampling areas, while I_{SERS} and I_{norm} are

Electronic Supplementary Information (ESI) for Journal of Materials Chemistry
This journal is © The Royal Society of Chemistry 2012

measured from the Raman spectra. Here, 1373 cm^{-1} and 1579 cm^{-1} were considered as the identification position for 2-NAT and 4-MBA, respectively. Assuming a molecular area of $0.22\text{ nm}^2/\text{molecule}$ for a thiol footprint in the SAM, the surface concentration of the SAM on silver or gold surfaces equals to $7.6 \times 10^{-10}\text{ mol/cm}^2$. Taking the sampling area (ca. $1\text{ }\mu\text{m}$ in diameter) into account, N_{surf} has a value of $5.9 \times 10^{-18}\text{ mol}$. For the solid sample, the sampling volume is the product of the area of the laser spot (ca. $1\text{ }\mu\text{m}$ diameter) and the penetration depth ($\sim 9\text{ }\mu\text{m}$) of the focused laser beam. On the basis of the density of bulk 2-NAT and bulk 4-MBA (both of 1.22 g/cm^3), the N_{bulk} values can be calculated to be $3.0 \times 10^{-14}\text{ mol}$ (2-NAT) and $3.2 \times 10^{-14}\text{ mol}$ (4-MBA), respectively.

3. Methanol electro-oxidation of Pt and Pd deposits

3.1 Electrode fabrication

After deposition on Al foils, Pt (Pd) catalysts were collected with centrifugation and washed with water, followed by removing the Al foils with H_2SO_4 solution. The catalyst ink was prepared by ultrasonically dispersing the catalyst powder in a 0.5 wt% Nafion ethanol solution with a concentration of catalyst about 2 mg ml^{-1} . A standard three-electrode cell was used at room temperature. A glass carbon electrode (GCE) as working electrode was modified by dropping 15 μl of the electrocatalyst ink. The counter electrode was a platinum wire and the reference was a saturated calomel electrode (SCE).

3.2 Methanol electro-oxidation

Fig. S-4A shows the typical cyclic voltammograms (CVs) of Pt and Pd catalysts, recording in 1.0 M KOH solution from -1.0 to 0.2 V at a sweep rate of 50 mV s^{-1} . There exist hydrogen adsorption/desorption peaks in the potential region -0.9 to -0.6 V . The electrochemical surface

Electronic Supplementary Information (ESI) for Journal of Materials Chemistry
This journal is © The Royal Society of Chemistry 2012

areas (ECSAs) were measured by integrating the charge on hydrogen adsorption–desorption regions by CV, and can be further calculated after the deduction of the double layer region on the CV curves represents the charge passed for the hydrogen desorption, Q_H , which is proportional to the ECSA value of the electrocatalysts. According to Fig. S-4A, the ECSAs were obtained for Pt (13.4 mC cm^{-2}) calatalysts and Pd (5.0 mC cm^{-2}) calatalysts.

The CVs of methanol oxidation on GCE electrode modified with Pt catalysts and Pd catalysts are shown in Fig. S-4B, which were recorded in $1 \text{ M KOH} + 1 \text{ M CH}_3\text{OH}$. Two peaks of methanol oxidation under condition can be clearly observed for the two catalysts: the oxidation peak in the forward scan corresponds to the oxidation of freshly chemisorbed species coming from methanol adsorption; the reverse oxidation peak is primarily associated with removal of carbonaceous species not completely oxidized in the forward scan. The magnitude of the peak currents on the forward scan indicates that the as-obtained Pt catalysts and Pd catalysts exhibited strong electrocatalytic activity for methanol oxidation.

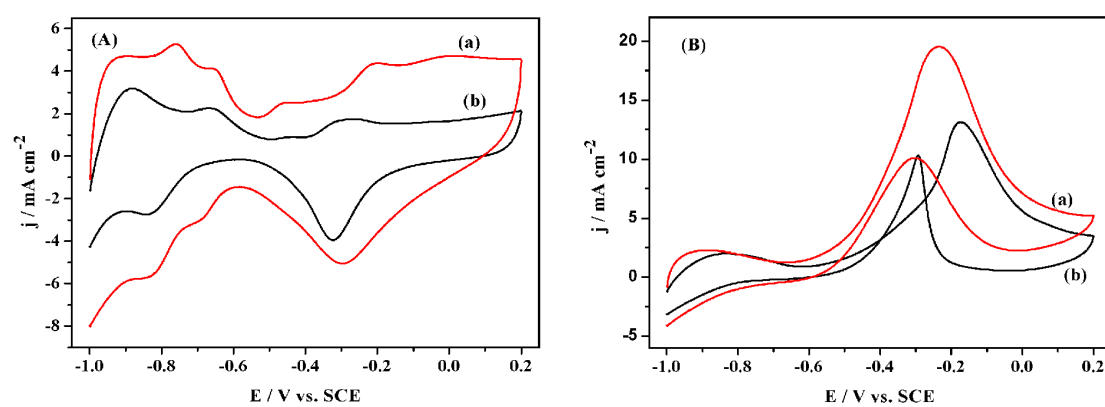


Fig. S4 Cyclic voltammograms in 1M KOH (A) and $1 \text{ M KOH} + 1 \text{ M CH}_3\text{OH}$ (B) on GCE electrode modified with Pt catalysts (a) and Pd catalysts (b), respectively. The scan rate was 50 mV s^{-1} .

Electronic Supplementary Information (ESI) for Journal of Materials Chemistry
This journal is © The Royal Society of Chemistry 2012

4. VSM test

To evaluate the magnetic properties of the as-deposited Co and Ni samples, Co and Ni particles were collected with centrifugation and washed with water, followed by removing the Al foils with H_2SO_4 solution. The static magnetic properties of sample were investigated by vibrating sample magnetometer (VSM, Lakeshore 7304), and parameters like specific saturation magnetization (M_s), coercive force (H_c) and remanence (M_r) were evaluated.

Magnetic hysteresis plots for Co and Ni deposits are shown in Fig. S-5A and S-5B, respectively. The hysteresis loops demonstrate that the samples of Co and Ni exhibit a soft ferromagnetic behavior at room temperature. The magnetic parameters including M_s , M_r and H_c , derived from the hysteresis plot, are given in Fig. S-5. The data reveal that the H_c of Co sample is larger than that of Ni sample. The M_s and M_r values of Co samples are also larger than those of Ni samples, respectively.

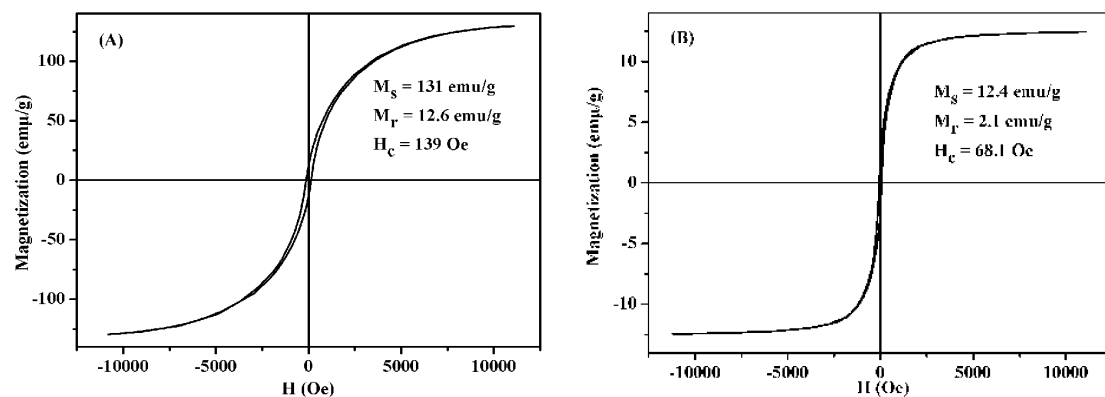


Fig. S5 Hysteresis loops of Co (A) and Ni (B) measured at room temperature.

Electronic Supplementary Information (ESI) for Journal of Materials Chemistry
This journal is © The Royal Society of Chemistry 2012

Table S1. The redox potentials of metallic ions³.

Couple	E^0 (V, vs. SHE)
Ag^+ / Ag	+ 0.799
$\text{AuCl}_4^- / \text{Au}$	+ 1.002
$\text{PtCl}_6^{2-} / \text{Pt}$	+ 0.744
$\text{PdCl}_4^{2-} / \text{Pd}$	+ 0.60
$\text{Cu}^{2+} / \text{Cu}$	+ 0.337
$\text{Co}^{2+} / \text{Co}$	- 0.277
$\text{Ni}^{2+} / \text{Ni}$	- 0.26
$\text{Zn}^{2+} / \text{Zn}$	- 0.763

References

- 1 M. Moskovits and J. S. Suh, *J. Phys. Chem.* 1984, **88**, 5526.
- 2 W.B. Cai, B. Ren, X. Q. Li, C. X. She, F. M. Liu, X. W. Cai and Z. Q. Tian, *Surf. Sci.* 1998, **406**, 9.
- 3 D. Walton and Nucleation, Marcel Dekker: New York, 1969.